VECTRI manual v1.6

Adrian Tompkins, ICTP, Trieste, Italy

Email: tompkins@ictp.it

Version release date: March 26, 2019
MOST DEFINITELY a work in progress

1 Prerequisites

The VECTRI code is a FORTRAN90 code with a bash shell script "wrapper" (in the process of being replaced by python3).

At the moment, in order to install and run it you will need to install the following libraries. In ubuntu this can be done using the `apt install` command:

git to download the files:

```
$ sudo apt get git
```

gfortran to compile the code

```
$ sudo apt get gfortran
```

The appropriate netcdf libraries

```
$ sudo apt get netcdf-lib
```

```
$ sudo apt get netcdff-lib
```

You will probably also find ncview and cdo useful for postprocessing and viewing the files:

```
$ sudo apt get cdo
```

```
$ sudo apt get ncview
```

More information on can be found on these external sites: https://code.mpimet.mpg.de/projects/cdo/climate data operators http://meteora.ucsd.edu/~pierce/ncview_home_page.htmlncview

NOTE TO WINDOWS USERS: These notes assume you are running the model on a linux system. If you are a windows 10 user, it is now possible to install native ubuntu (or other linux flavours) directly under windows, without the need for cygwin or a wine server. There are many online blogs that show you how to do this. We strongly recommend that you install linux under windows which will then enable you to easily install the above software and run the model (we have successfully done this at a number of workshops and training events).

For use at ECMWF, there is also the option for using a GRIB input/output interface instead of netcdf, but most users will rely on the standard interface.

2 Downloading the code

Before you run the code familiarise yourself with the concept of directories and subdirectories in your file system. When you want to use VECTRI there are two directory locations that are important, the one where you STORE the code and the one where you RUN the code.

NOTE: As the code is managed using the repository software git https://git-scm.com/ you never want to run the code in the directory or subdirectory of the code location, to avoid making lots of files that git will think are part of the code! In fact the code script tries to detect and prevent this occurrence.

We suggest that you place the code in a location such as

`$HOME/vectri`

and run it somewhere in parallel such as

`$HOME/myruns`

To get the code, change to the parent directory where you want to host the code, e.g.:

`cd $HOME`

and then retrieve a copy. The VECTRI code is hosted on gitlab at the moment. You can download a copy from the gitlab repository:

`$ git clone https://gitlab.com/tompkins/vectri.git`

This should give you the message:

`Cloning into 'vectri'...`

along with some additional messages. After if you list your directory contents with `$ ls` you should see a subdirectory called vectri.

Now there is one thing we need to do before we start, and that is to set up an environmental variable that points to the code. This is so, no matter where you run, the scripts know where to find the code. This will depend on the flavour of shell you use:

ksh or bash: `$ export VECTRI=directorylocation`

csh: `$ setenv VECTRI directorylocation`

(note UPPER CASE "VECTRI" is important). So if your code is in $HOME/vectri and you use bash then you need to type

`$ export VECTRI=$HOME/vectri`

test it by typing

`$ ls $VECTRI`

and you should see:

`data doc LICENSE README.txt scripts source utils vectri`

If instead you get a blank response, you haven't followed the steps above correcly. Now to be convenient, you don't want to do this each time you log in to a new konsole shell, so it is best to find out which start up file your system reads in your $HOME, (.kshrc, .login, .profile, etc) and place this command there. Test it by opening a **new** shell and typing

```
$ ls $VECTRI
```

and you should see:

```
data doc LICENSE README.txt scripts source utils vectri
```

3 Running the code

From v1.5 the interface has been simplified massively. The code no longer supports text input/output and only allows netcdf intput. But first where do you want to run? Just make a run directory and go there! e.g.

```
$ mkdir -p /scratch/tompkins/vectri/
```

```
$ cd /scratch/tompkins/vectri/
```

Now we are ready to run. The driver script for vectri is simply called vectri! If we call this script without arguments we get a helplist of instructions, let's try it (note that we need to use the $VECTRI path, but you can set up your own bash alias to point to the driver programme if you like):

```
$ cd $VECTRI/vectri
```

This should return the following message:

```
+++ welcome to /afs/ictp/home/t/tompkins/vectri/vectri
```

```
vectri usage
```

From version 1.5 in Feb 2019 the code has a simplified interface

- the code only needs to have the names of the external files

-h –help : print this usage message

-c –climfile : climate file name (can be grib or netcdf) - auto detect from .grb/.nc

-d –datafile : netcdf data file containing

population (mandatory) - varname population/pop permanent breeding fraction (optional) - varname wperm

land use category (optional) - varname lu/luc

-o –outfile : output filename (default vectri.nc)

-i –initfile : initialization file or init option

```
 -g --grib :  force climfile format to be considered grib (default
is netcdf otherwise if not .grb)
```

Now if you look in the data directory you will find that there are a some example files with which you can try to run vectri:

```
$ ls $VECTRI/data/*.nc
```

will reveal two files, take a look at them with ncview if you like:

```
vectri_fake_clim.nc vectri_fake_data.nc
```

One is a fake climate file and the other a fake data file.

Run vectri using these files as input:

```
$ vectri -c $VECTRI/data/vectri_fake_clim.nc -d $VECTRI/data/vectri_fake_data.nc
```

This should compile and run the model.

NOTE: the makefile that does the compilation step is found in $VECTRI/scripts/makefile and it assumes that all the libraries for netcdf etc are installed in standard locations (e.g. /usr/lib) - If you have a non-standard installation for libraries you may need to edit this file to point to the correct system locations

4 Output

After running you will find two directories input and output. The main output file is called *vectri.nc* which is found in the subdirectory `output` after each successful run (unless you chose to rename it with the -o option). The file is in standard netcdf format and you can use two commands to examine its content `ncview` and `ncdump`.

ncdump outputs the entire contents of a file, perhaps a little more than you bargained for, so use the useful option `-h` to examined the file *header*. The command lets us know the dimensions of the output, gives a list of the model output variables, as well as their *metadata*. Lastly, but certainly not least, the dump provides a list of all the model run *global attributes*. Here you find stored all of the run parameters. Many of these can be set by the user, so it is very useful to have a record *inside the file*! We could dump a individual variable using the `ncdump -v variable` command, but it is also possible to graphically interrogate the file using ncview.

Using the command `ncview ./output/vectri.nc` launches the graphical viewer. There is a panel containing a list of variables. Clicking on one of these variables launches a display window (Fig. 1). If you conducted a gridded regional integration then you will get a map of the output, otherwise you will get a line graph for a station integration The input variables of population, temperature and rainfall are stored in the file.

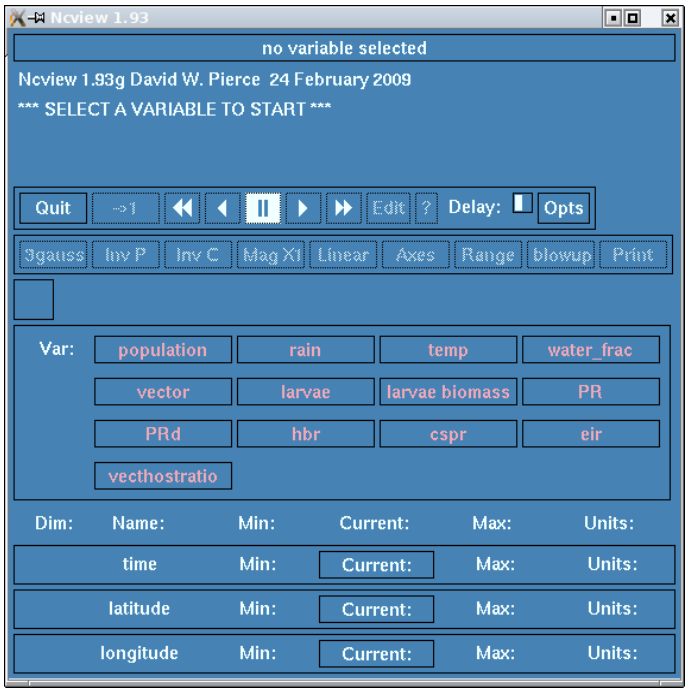

Figure 1: An example ncview window showing vectri output

Table 1: The Vectri output (some of these are optional and switched off my default)

name	definition	units
population	population density	km^{-2}
rain	rainfall	mm day^{-1}
temp	temperature	deg C
water_frac	fraction of grid box covered by pond breeding sites	
vector	mosquito density	
larvae	larvae density	
larvae_biomass	larvae biomass	mg m^{-2}
PRd	proportion of population with detectable malaria (day 10+)	
hbr	human bite rate	number $person^{-1}$ day^{-1}
cspr	Circum sporozoite protein ratio (fraction eir/hbr)	
eir	entomological inoculation rate (number of infectious bites)	number $person^{-1}$ day^{-1}
vecthostratio	ratio of mosquitoes to people	
cases	Number of clinical cases	fraction
immunity	Proportion of population with full clinical immunity	fraction

5 Setting options in VECTRI

It is possible to set options in VECTRI. This is done in the file *vectri.options* which you should save in the sub-directory **input**.

vectri.options

You may open the file vectri.options using the text editor of your choice (e.g. *emacs ./output/vectri.options*. The file is empty by default, but you can enter a list of parameter values to control vectri, which must be separated by a comma. You may put each parameter on a new line for clarity if you wish:

parameter1=value,

parameter2=value,

The parameters you may specify are given in the follow tables, which associate parameters according to themes:

6 Making the input from csv data

There is a new script in v1.5 which allows you to make input files from csv data or by specifying constant values. To get the help type

```
$ $VECTRI/utils/vectri_point_input --help
```

Commonly you will want to convert a txt or csv file into a netcdf input file, usually specifying a fixed value for population density. (NOTE, at the moment the text file is space not comma separated).

So if you look at the text example file:

```
$ less $VECTRI/data/vectri_fake_clim.txt
```

you will see it has 1 header line, and the year in column 2, month in col 3, day in col 4 followed by mean temperature and rainfall. Thus the command to convert this to netcdf with a population density of 100 per km2 would be

```
$ $VECTRI/utils/vectri_point_input --nhead 1 --cyyyy 2 --cmm 3 --cdd
4 --ctmin 5 --ctmax 5 --crain 6 --pop 100 --rain $VECTRI/data/vectri_fake_clim.txt
--temp $VECTRI/data/vectri_fake_clim.txt
```

you can set the output names with –climfile and –datafile if you like

NOTE: new script, likely to subject to bugs, please report

Table 2: run control parameters

parameter	definition	default	units
nyearspinup	length of spinup period discarded from output	0	years

Table 3: larvae parameters (version 1.26)

parameter	definition	default	units
neggmn	eggs laid per female vector	120	
nlayingmax	maximum number of vectors allow to lay (-ve no limit)	-99	
rlarv_tmax	maximum temperature for larvae survival	35	deg C
rlarv_eggtime	time for egg hatching	1.0	days
rlarv_pupaetime	time for pupae stage	1.0	days
rlarv_flushmin	minimal daily survival L1 larvae after intense rainfall	0.4	
rlarv_flushtau	exponential decay of flushing with rainrate	50	mm day^{-1}
rmasslarv_stage4	mass of L4 larvae	0.45	mg
biocapacity	larvae biomass carry capacity of pools	300	mg m^{-2}
rlarvsurv	base survival rate due to preditation	0.825	

Table 4: larvae parameter (version 1.3)

parameter	definition	default	units
neggmn	eggs laid per female vector	80	
nlayingmax	maximum number of vectors allow to lay (-ve no limit)	-99	
rlarv_tmin	minimum temperature for larvae survival	16	deg C
rlarv_tmax	maximum temperature for larvae survival	37	deg C
rlarv_eggtime	time for egg hatching	1.0	days
rlarv_pupaetime	time for pupae stage	1.0	days
rlarv_flushmin	minimal daily survival L1 larvae after intense rainfall	0.4	
rlarv_flushtau	exponential decay of flushing with rainrate	50	mm day^{-1}
rmasslarv_stage4	mass of L4 larvae	0.45	mg
biocapacity	larvae biomass carry capacity of pools	300	mg m^{-2}
rlarvsurv	base survival rate due to preditation	0.825	

Table 5: hydrology (version 1.26, a new beta scheme is available in 1.3)

parameter	paper	definition	default	units
ipud_vers		puddle parametrization version (125/126/130)	126	
rwaterfrac_perm	w_0	permanent breeding site fraction	10^{-6}	
rwaterfrac_max	w_{max}	maximum coverage by breeding sites	0.04	
rwaterfrac_rate	K_w	pond geometry factor	10^{-3}	mm^{-1}
rwaterfrac_evap126	$E + I$	infiltration and evaporation rate loss of ponds	250	mm day^{-1}
rwater_tempoffset	T_{wat}	temperature offset of pond to air	0	deg C

Table 6: interventions

parameter	definition	default	units
rnobednetuse	proportional of host NOT using bednet	1	
rbednettreat (INOPERATIVE)	proportion of bednets insecticide treated	0.0	

Table 7: biting parameters

parameter	definition	default	units
rzoophilic_tau	e-folding population density for zoophilicity rate	50^{-4}	m^{-2}
rzoophilic_min	minimum anthropophilic bite rate at low population densities	0.1	
rbiteratio	bite rate success	0.6	per day

Table 8: gonotrophic and sporogenic

parameter	definition	default	units
rtgono	threshold temperature for egg development in vector	7.7	deg C
dgono	degree days for egg development in vector	37.1	days
rtsporo	threshold temperature for parasite development	16.0	deg C
dsporo	degree days for for parasite development	111	days

Table 9: population

parameter	definition	default	units
rpop_growth	population growth rate	1.0	ratio per year
rpopdensity_min	minimum population density considered	10^{-6}	m^{-2}
rmigration	simple migration fraction imported cases	0.0	$year^{-1}$

7 Model Description

The malaria model presented is a grid cell distributed dynamical model and is referred to as VECTRI; the *vec*tor borne disease community model of the International Centre for Theoretical Physics, *Tri*este[1]. In as far as possible, the model physics and associated parameters are taken from the literature for the *Anopheles gambiae* complex and the Plasmodium falciparum malaria parasite. In the present version each location (grid cell) is independent, but the structure of the model will allow communication between grid cells such as vector flight or human population migration to be easily incorporated. The following sections describe the basic structure of the model, with emphasis placed on its novel aspects.

Since one goal of the model is its successful application regionally to forecast epidemic outbreaks in malaria marginal zones in addition to representing malaria transmission in endemic regions, it is important to represent the delay between the rainy season onset and the malaria season. Thus the model explicitly resolves the growth stages of the egg-larvae-pupa cycle in addition to the gonotrophic and the sporogonic cycles using an array of bins for each process, similar to the LMM. The structure of the model is depicted schematically in Fig.1. It shows the division of the larvae life cycle (L) into a number (N_L) of discrete fractional bins (i). The real number stored in each bin, L_i, gives the larvae density (per square metre) at a particular fractional growth stage f (where f ranges from 0 to 1). Oviposition results in eggs added to the first bin and each timestep of the model larvae advance a number of bins at a fractional growth rate R_L (units

[1]This manuscript documents VECTRI release version v1.25 as of June 2012

Table 10: toy climate

parameter	definition	default	units
rtemperature_offset	temperature offset	0.0	deg C
rtemperature_trend	temperature trend	0.0	deg C yr $^{-1}$
rrainfall_factor	ratio to scale rainfall by	1.0	

s^{-1}), depending on the local water temperature, until they reach the final bin (representing $f = 1$) and develop into adult mosquitoes. The equations solved are thus the classic advection equation:

$$\frac{dL}{dt} = R_L \frac{dL}{df}. \tag{1}$$

The vector status is also bin resolved, consisting of two properties: the gonotrophic and sporogonic cycles. It is thus represented as a two dimensional array $V(N_{gono}, N_{sporo})$. All vectors in the first gonotrophic bin $\sum_{j=1}^{N_{sporo}} V(1, j)$ are in meal-searching mode, and once a meal is obtained, the vectors advance in terms of the egg development state at a rate $R_{V,gono}$ related to ambient temperature until the final bin is reached (using the advection equation similar to eqn. 1). At this point the vector lays a new raft of eggs and is recycled to the first meal-searching bin.

Each timestep, parasite transmission may occur to a proportion of the biting vectors, and the status of these vectors will subsequently additionally progress in the sporogonic dimension, with the rate $R_{V,sporo}$ again determined by temperature. Once vectors reach the final bin they are infective to humans and remain so until death. A third array of bins maps the status of the disease in the human host (H) population (dimension N_H), with the first bin representing the uninfected population. The model does not include age or immunity factors, which is the subject of present model development.

Thus, while the model introduces new relationships regarding the surface hydrology and the explicit interaction between vector and host, the underlying numerical structure is similar to that employed in the LMM [1]. A timestep of one day is used to integrate the model equations, although a shorter timestep could be used if input data (temperature/rainfall) are available on these timescales, and the advection equation is solved using a simple upstream numerical scheme.

The model can be flexibly integrated using a wide range of horizontal resolutions. Since the model presently does not permit vectors to move to neighbouring grid cells, the model resolution is limited to an upper (finest) level on the order of 1-5 km; an indicated range below which mosquito movement can become significant [2, 3, 4]. Integrating the model at O(10km) resolution is desirable, even if corresponding observational data of clinically proven malaria cases is available only on coarser scale health districts. This is because malaria transmission is a highly nonlinear function of its drivers such as climate and land surface and thus it is preferable to use highest possible spatial resolution inputs of population density, land surface and weather to account for this, while the model output is subsequently aggregated to the spatial scale at which health data is available for comparison.

The following section describes the details of the parametrizations used to describe the temperature-sensitive progression rates and details the new developments in the VECTRI model concerning the representation of the human population density, which impacts the biting rates, and the treatment of surface hydrology which determines the overall vector number. To enable VECTRI to be used in a multi-model ensemble approach to assess model uncertainties,

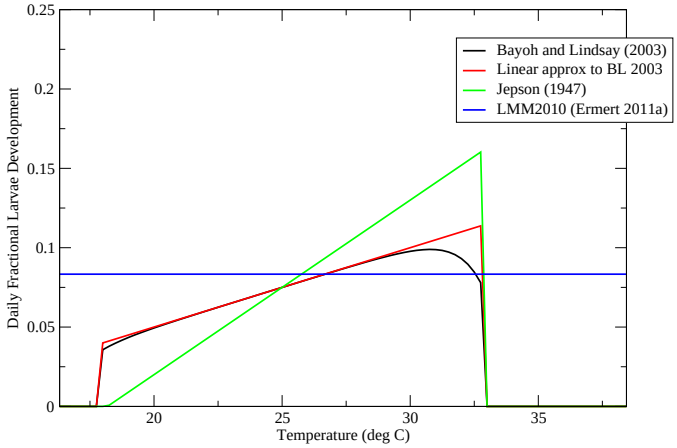

Figure 2: Larvae development rates as a function of temperature as modelled by [7](black/red), [6](green) and [8](blue). All three linear forms are implemented in VECTRI.

multiple parametrization choices are incorporated to facilitate this. All the constants are listed in table 1.

7.1 Larvae cycle

Previous laboratory studies have shown that the larvae growth rate follows the degree day concept [5] based on a linear function of water temperature T_{wat} above a threshold value $T_{L,min}$ below which larvae growth ceases:

$$R_L = \frac{T_{wat} - T_{L,min}}{K_L}. \tag{2}$$

There is considerable uncertainty in the setting of the rate coefficient K_L , however, with [6] K_L value of 90.9 degree days, while a linear approximation of the relationship derived by [7] results in a much slower rate of 200 degree days. A further source of uncertainty is the specification of the water temperature itself, which depends on the shading of the pool and its dimensions in addition to the ambient air temperature, and is described in the hydrology component below. VECTRI also permits the user to avoid this uncertainty by following [8] in setting a fixed larvae growth rate (i.e. independent of T_{wat}) to have a cycle of 12 days, the default option selected. The sensitivity to this relationship is investigated later. Irrespective of the scheme used, an upper temperature limit $T_{L,max}$ is specified above which larvae death occurs.

Egg hatching into larvae and the pupae development stage are both typically on the the order of one day [9, 7] and thus are poorly resolved by the daily

timestep employed by VECTRI and other similar dynamical models. In order to avoid truncation problems the length is fixed in VECTRI to last exactly one day and is temperature independent.

7.2 Larvae mortality

The mortality rate of larvae is an important factor for transmission, and is strongly temperature dependent [10]. The VECTRI model sets a base daily survival rate for larvae $P_{L,surv_0} = 0.825$ taken from [8], slightly lower than the values given by [1, 11]. Development of larvae is negatively affected by larvae over-population due to competition for resources [12]. This is incorporated in VECTRI by reducing survival rate proportionally by a factor related to resource constraints:

$$P_{L,surv} = \left(1 - \frac{M_L}{wM_{L,max}}\right) K_{flush} P_{L,surv_0}. \tag{3}$$

In the first term on the right, M_L is the total larvae biomass per unit surface area of a water body, and w is the fraction coverage of a grid cell by potential breeding sites (not open water) and is given by the surface hydrology component described below. If $w = 0$ the survival rate $P_{L,surv}$ is also zero. The maximum carrying capacity, $M_{L,max}$, is set to 300 mg m^{-2} and larvae mass is assumed to increase linearly with a stage 4 larvae having a mean mass of 0.45 mg, both following [13, 11] closely. All larvae die above a water temperature of $T_{L,max}$.

Flushing of larvae by heavy rainfall has been suggested to be an important cause of larva mortality [14, 15]. Using an artificial pond apparatus [16], a 17.5% daily mortality rate of first stage larvae reducing to 4.8% for forth stage larvae was estimated, although the authors state that these figures could represent an underestimate due to the symmetry of the pond apparatus and the lack of sampling of more extreme rainfall amounts during the experiment campaign. On the other hand, vegetation in natural pools and the apparent ability for *Anopheles gambiae* larvae to take avoidance measures to avoid flushing could imply a lower flushing rate [17]. In order take the simplest possible relationship in VECTRI, flushing rate is represented as exponential function of rate rate, and is related linearly to the larvae fractional growth state L_f:

$$K_{flush} = L_f + (1 - L_f)\left((1 - K_{flush,\infty})e^{\frac{-R_d}{\tau_{flush}}} + K_{flush,\infty}\right), \tag{4}$$

where R_d is the rainfall rate in mm day^{-1}, τ_{flush} describes how quickly the effect increases as a function of R_d, and $K_{flush,\infty}$ is the maximum value of K_{flush} for newly hatched first stage larvae at extremely high rain-rates. In contrast the flushing effect is zero ($K_{flush} = 1$) at all rain rates for stage 4 larvae just prior to adult emergence ($L_f = 1$, corresponding to the larvae bin $i = N_L$). The relationship is illustrated in Fig.2. Since flushing is a function of daily rate rate at relatively high spatial resolution τ_{flush} is set to 50 mm day^{-1}. In order to give mortality rates of first stage and forth stage comparable to [16] for typical daily rain rates in the tropics, a value of 0.4 is adopted for $K_{flush,\infty}$.

Table 11: Larvae scheme parameters

parameter	definition	default	units
nlarv_scheme	larvae water temperature scheme (1,2,3) 1=ermert:2011a,2=jepsen47,3=bayoh lindsey 2003	1	
nsurvival_scheme	mosquito survival temperature scheme (1,2,3) 1=MartinsI,2=MartinsII,3=Bayoh(not yet!)	2	

7.3 Gonotrophic cycle

All female vectors are assumed to find a blood meal in the first night of searching, although this fraction can be set as a model parameter. Insecticide treated nets are, for example, able to frustrate host-seeking mosquitoes [18]. The introduction of a fraction of emerging mosquitoes would reduce the mosquito population number. It would depend on the human populationand availabilityof animals. Not only newly emerging mosquitoes seek to find a blood meal also adult mosquitoes might not be able to progress in the feeding cycle.

Once the blood meal is taken, the egg development proceeds at a rate determined by the local 2 metre air temperature T_{2m}, again following the degree day concept and is thus given:

$$R_{gono} = \frac{T_{2m} - T_{gono,min}}{K_{gono}}. \tag{5}$$

At the end of the cycle the female vector lays N_{egg} eggs that will eventually hatch into females; as is usual in such models, the eggs laid that result in the males are neglected. She subsequently cycles to the meal searching box. The number of eggs is highly variable and likely depends on vector species. The choice of N_{egg}=120, corresponding to a batch size of 240 assuming equality between the sexes, follows [19] but [20, 21, 22] indicate that this could be an overestimation. Present model development underway will permit stochastic variation of parameters such as N_{egg} in the future to account for their considerable degree of uncertainty in an ensemble modelling framework.

7.4 Sporogonic cycle

When the female vector takes a blood meal there is a certain finite probability that malaria transmission takes place, either from the host to vector or vice versa. The probability of transmission to the vector during a blood meal from an infective host is considered a constant $P_{hv} = 0.2$ (following [8]), and thus the overall transmission probability $P_{h\to v}$ is the product of P_{hv} and the proportion of hosts that are infective, namely the ratio of the population density of infected hosts H_{inf} divided by the population density H:

$$P_{h\to v} = \frac{H_{inf}}{H} P_{hv}. \tag{6}$$

It should be noted that this assumes bites are randomly taken and not influenced by the host's infective state. Heterogeneous biting can impact the basic reproductive number considerably [23, 24]. Heterogeneity of feeding habits is

related to a wide array of factors, including host attractiveness to the vector and their vicinity to breeding sites, and heterogeneity in interventions such as the use of bednets, in particular the increased use by host suffering from clinical malaria. Some of these effects could easily be included in VECTRI if relevant data were available.

Each timestep, a proportion of vectors $P_{h\to v}$ become infected, and the parasitic development in the midgut of the vector begins, once again governed by a degree day concept:

$$R_{sporo} = \frac{T_{2m} - T_{sporo,min}}{K_{sporo}}. \tag{7}$$

After a number of days the sporozoites invade the salivary glands of the mosquito which subsequently becomes infective to humans. The mosquito is assumed to remain in this infective state until its death.

7.5 Vector survival

In addition to the larvae, gonotrophic and sporogonic cycles, temperature also plays a role in determining the mortality of vector. High air temperatures increase vector mortality, but the relationship is uncertain, especially at the high and low temperature bounds of transmission. As in the larvae cycle, two schemes are incorporated in the VECTRI model to permit a multi-model approach, with constants given in table 1:

Scheme 1: follows [25, 14] and gives the survival rate as a quadratic function of temperature:

$$P_{V,surv1} = K_{mar1,0} + K_{mar1,1}T_{2m} + K_{mar1,2}T_{2m}^2 \tag{8}$$

Scheme 2: follows [26, 27], revising the relationship as

$$P_{V,surv2} = exp\left(\frac{-1.0}{K_{mar2,0} + K_{mar2,1}T_{2m} + K_{mar2,2}T_{2m}^2}\right) \tag{9}$$

The results in this paper are obtained using scheme 2, referred to in [19] as *Martens II*.

7.6 Indoor Temperatures

The model introduces the indoor temperature parameterization of [28]:

$$T_{indoor} = T0 + KT_{2m} \tag{10}$$

where Lunde suggested T0=10.33^{o}C and K=0.58. The user can specify which proportion of time the vector spends indoor resting with the factor β_{indoor} (in code: rbeta_indoor), which is set to **zero** by default. The temperature the vector is exposed to is then a weighted mean:

$$T = \beta_{indoor}T_{indoor} + (1 - \beta_{indoor})T_{2m} \tag{11}$$

7.7 Host community

One of the new aspects of the VECTRI model is that is explicitly allows the interaction between vector and host population on a district and regional scale. The VECTRI model specifies the population density H using the Africa-only AFRIPOP [29] or global GRUMP [30] datasets which have a nominal 1 km and 4.5 km spatial resolution, respectively. Thus at each location (model spatial grid cell), the ratio of biting vectors to hosts is known and is given by $(\sum_{j=1}^{N_{sporo}} V(1,j)/H)$. This is important to represent the vector-to-host transmission rate. The number of bites B that any particular individual receives in a given time the human biting rate (hbr) is considered to be a random process, and thus distributed following a Poisson process with a mean biting rate of

$$\overline{hbr} = \left(1 - e^{\frac{-H}{\tau_{zoo}}}\right) \frac{\sum_{j=1}^{N_{sporo}} V(1,j)}{H}. \tag{12}$$

The factor $1 - e^{\frac{-H}{\tau_{zoo}}}$ represents the level of vector zoophilly. While members of the *Anopheles gambiae* complex are in general considered anthropophilic to varying degrees [31], with *arabiensis* more zoophilic than *sensu stricto* [32], vectors take an increasing proportion of blood meals from cattle in lower population density rural areas with high livestock numbers [33], although the effectiveness of zooprophylaxis is still debated [34]. The exponential factor reflects this, with the e-folding population density for the effect set to τ_{zoo}=50 km^{-2}. Thus the factor only has a significant impact for rural populations below this number and avoids the model producing excessively high biting rates and EIR for sparsely populated locations. In future, VECTRI will allow vector movement between cells allowing anthropophilic vectors to cluster around population centres.

The daily number of infectious bites by infectious vectors, EIR_d, is the product of hbr and the CircumSporozoite Protein Rate, $CSPR$. Specifically in the VECTRI notation, this is $V(1, N_{sporo})/H$, with the 1 indicating that the calculation is restricted to the vectors that are biting within the present timestep of the model. This implicitly assumes that there is no change in the intensity of biting or the gonotrophic cycle length between uninfected and infectious vectors; a simplification according to [35]. If the transmission probability from vector to host for a single bite of an infective vector, P_{vh}, is assumed a constant (VECTRI adopts a value of 0.3 [8]) then the transmission probability for an individual receiving n infectious bites will be $1 - (1 - P_{vh})^n$. The impact on transmission due to blocking immunity is neglected. Thus the overall transmission probability per person per day in the model can be obtained by integration the over the bite distribution:

$$P_{v\to h} = \sum_{n=1}^{\infty} G_{\overline{EIR_d}}(n)\,(1 - (1 - P_{vh})^n) \tag{13}$$

where $G_{\overline{EIR_d}}$ is the Poisson distribution for mean $\overline{EIR_d}$. If bednets are in use, eqn. 13 could be modified to incorporate this, increasing the mean bite rate for a subset of the unprotected population. This involves a number of complications however, since accurate data would be required concerning bednet distribution and use, how this usage correlates to host infective state, and which proportion of bite are taken during the hours of sleeping.

There is a differential mean bite rate for hosts in the exposed, infected and recovered (EIR) individuals relative to the susceptible category (S), to produce over dispersive biting rates and reflect the fact that some individuals are more attractive to vectors [36, 37, 38], are more vulnerable due to clothing and housing standards[39], access to nets, location of housing with respect to water bodies [40, 41, 42], and that parasite infection also appears to increase attractiveness of individuals to vectors [43], although the latter effect is offset by increased net use in the case of clinical symptoms. anthrophic vectors

The impact of using eqn. 13 is to reduce the mean transmission rate, particularly when the mean bite rate is small resulting in a strong positive skewness of the Poisson distribution (Fig. 3). While this is an improvement on the simple assumption that all hosts receive equal numbers of bites, the Poisson distribution is likely under-dispersive compared to reality, since a number of factors such as unequal host attractiveness to vectors and nocturnal behaviour affecting exposure will likely lead to a uneven distribution of bites rates [44, 37, 38]. Fig. 3 also emphasizes that the model is relatively insensitive to the choice of P_{vh} for values exceeding around 0.2.

The host population is represented by the vector $H(N_{host})$, and each VECTRI timestep a proportion $P_{v\rightarrow h}$ of hosts become infected and progress through the array until 20 days later they assume an infective status, an average value for immune and non-immune subjects [45, 46, 47, 48]. Non-immune hosts clear infections at an e-folding rate of $C_{ni} = 150$ days. Even after a century of study of the disease, the paradigm of naturally acquired immunity (NAI) is still hotly debated [49]. Therefore the present version of the model neglects host immunity, and the impact of the various representations of immunity in VECTRI will be the subject of a companion article.

PARAMETER TABLE

7.8 Immunity

from v1.4 host immunity was added to the model. host immunity has been added in a simple SEIR approach to the original model, using a scheme that closely follows [50]. In the default immunity scheme, immunity is gained as a result of infectious bites, with an e-folding scale set such that 95% of individuals receiving 100 infectious bites per year (EIRa=100) will be clinically immune [51, 49]. A Newtonian relaxation loss term is applied so that 95% of individuals lose immunity after 3 years. In addition to clinical immunity, the model also accounts for transmission blocking immunity in the same way as [52, 50], by reducing the host to vector transmission probability in immune individuals [53], (and see review in supplementary tables 5 and 7 in [8]).

7.9 Surface hydrology

The VECTRI model includes a simple, physically-based surface hydrology model that at each timestep provides a calculation for the fractional coverage of each model gridcell by potential breeding sites for the malaria vector, w. This fraction

Table 12: immunity and transmission parameters

parameter	definition	default	units
rhostclear	clearance rate for non-immune adults	150	days
rpthost2vect	probability of infected transmission from infected host to vector	0.2	
rptvect2host	probability of infected transmission from infected vector to host	0.3	
rimmune_gain_eira	Annual EIR required to gain full immunity	100	bites ppp
rimmune_loss_tau	E-folding timescale for immunity loss	365	days
rpop_death_rate	dead and replacement rate	0.02	fraction
rpopdensity_min	minimum population density for code to run	5e.-7	per km^{-2}
rbitehighrisk	ratio of rate of bites for high risk (E) to low risk (S) categories	5	

consists of two components since the model distinguishes between breeding sites provided by temporary ponds, w_{pond}, and those associated with permanent water bodies such as lakes, rivers and streams that contain water year-round, w_{perm}:

$$w = w_{perm} + w_{pond}. \tag{14}$$

Considering first w_{perm}, converting land use and terrain information into a fractional coverage of breeding areas provided by permanent water bodies is a significant challenge. Wave/ripples action that can drown larvae [54] and the presence of predators in larger bodies [55] imply that larvae exist only in a sub-fraction of such water bodies, in pooling that occurs on the edges of lakes and rivers or the shallow edges of ponds. Higher soil moisture in the vicinity of large water bodies can boost available breeding sites by reducing infiltration loss and increasing the lifetime of temporary puddles and ponds. Lastly, rivers and streams can even confound classic relationships between rainfall and vector density by actually providing more breeding sites during drought periods when flow slows or stops altogether [56]. This remains the subject of current research and the default VECTRI model therefore sets w_{perm} to zero in each grid cell, implying that the breeding site availability is dominated by seasonal ephemeral ponds and malaria incidence will be potentially underestimated in the vicinity of larger semi-permanent water bodies. A user operating the model for a local area with knowledge of permanent water bodies can set this value appropriately.

The net aggregated fractional coverage by temporary pools w_{pond} is derived from a simple water balance model. Ponds are replenished by surface runoff Q, while infiltration I (seepage) and evaporation E and pond overflow reduce their water content. An important parameter is the maximum coverage of the temporary ponds w_{max}, which described the extent of depressions that could potentially become water filled at the peak of a wet season, which are often small in scale, with total catchments of the gully systems studies in Niger in the HAPEX-SAHEL experiment measuring 0.2 km^{-2}. Presently is assumed that the runoff Q that fills the ponds mostly falls within these depressions and thus the run off is set to $Q = w_{max}P$. Thus sub-surface infiltration occurring within the depressions is also considered a water source for temporary pools [57]. Future developments will introduce improved runoff treatment accounting for soil texture and slope.

The source from precipitation is balanced by evaporative, infiltration and overflow losses. In high resolution simulations of surface hydrology in Niger, [58]

found overflow losses to be approximately 20% of total losses, more than three times the losses due to evaporation. It should also be noted that overflow losses in field campaigns are difficult to measure and thus are often incorporated in the infiltration, which is calculated as a residual in the water balance calculation. Losses through pond overflow are assumed to increase linearly with pond fraction in VECTRI, achieved by scaling the runoff by a factor $1 - \frac{w_{pond}}{w_{max}}$. Once the pond fraction reaches its maximum, all surface runoff overflows and is lost. Infiltration losses vary substantially depending on soil texture and life-scale of the pond in question. Often the infiltration is a highly nonlinear function of water body extent, since silting may significantly reduce infiltration in the lowest part of longer-lived or semi-permanent pools [57]. This results in a fast initial decay after rain events due to high infiltration rates at the pool edges, followed by a slower decay, while temporary, shorter lived water bodies tend to have more uniform infiltration rates. These rates can be very high, exceeding 600 mm day^{-1} [59]. Presently the VECTRI model simply sets a fixed constant infiltration rate per unit pond area.

Combining these factors, the volume of water v_{pond} in ponds per unit area thus evolves as

$$\frac{dv_{pond}}{dt} = (w_{max} P(1 - \frac{w_{pond}}{w_{max}} - w_{pond}(E + I)). \tag{15}$$

Evaporation is set to 5 mm day^{-1}, equivalent to a latent heat flux of 145 Wm^{-2}. It is possible to derive evaporation losses from water temperature, and atmospheric wind speed and relative humidity, however, as evaporation is a relative minor loss term relative to infiltration and overflow, a simple fixed evaporation rate suffices. With I set to a reasonable value of 245 mm day^{-1}, total losses from infiltration and evaporation are thus 250 mm day^{-1}. For closure, the pond fractional coverage needs to be related to the volume. Individual ponds have been modelled previously using a power law approximation [60], which would lead to a relationship $\frac{dw}{dt} \propto w^{-p/2} \frac{dv}{dt}$, where p is the power law exponent. However, [60, 61] show that p can vary by almost an order of magnitude from one water body to another and depends in particular on the life-time. In the present version model, this factor is presently neglected and the coverage is simply linearly related to volume introducing a tunable factor K_w:

$$\frac{dw_{pond}}{dt} = K_w \left(P(w_{max} - w_{pond}) - w_{pond}(E + I) \right). \tag{16}$$

As the pond coverage can change rapidly, eqn. 16 is integrated using a fully implicit solution. An example evolution of the fractional pond coverage for a site near Bobo Dioulasso is given in Fig. 4, which shows that the simple empirical approach mimics the pond evolution modelled by high resolution hydrological models for sites in Niger [11] and ponds modelled in Senegal [62]. The present empirical formulation is similar to the approaches of [63, 64]. It is seen that at the fringes of the rainy season, puddles and small ponds have limited longevity on the order of a few days, implying that they are unsuitable for vector breeding. VECTRI represents the bulk behaviour of ponds, rather than the ultra-high resolution model of [58] which individual models puddles at the 10 m scale and thus can model the lifetime of ponds as a function of their explicit size (see their figure 7). Obviously, the linear relation between rainfall and the growth of potential breeding sites in parameter K_w is a simplification, while the other

terms should be related to atmospheric conditions, soil type, vegetation coverage and terrain slope demonstrated to be important for malaria transmission in the Kenyan highlands [65].

Presently, the two unknowns w_{max} and K_w in the framework are set using a simple Monte Carlo suite of station data integrations in a subset of locations to minimize EIR errors compared to field data. An example sensitivity integration is shown in Fig. 5, which is a integration conducted for Bobo Dioulasso using station data to drive the model (see below for experimental set up details). It is seen that transmission intensity increases with w_{max} and K_w as expected, since these increase the pond coverage for a given rainrate, while increasing the loss rate acts in the opposite direction. For a given station there are a range of reasonable parameter values, with the present parameter settings chosen using a small number of locations in west Africa. Nevertheless, the physically based framework facilitates future improvement currently underway, which will include direct validation of the revised hydrological model constants using in situ and remotely sensed data.

Finally, it is recalled that the pond dimension limits larvae mortality rates through the availability of breeding sites governed in eqn. 3. This is an approximation of the net affect of crowding which leads to higher mortality rates, longer development times and smaller adults [66], which in turn have a competative disadvantage [22]. The biomass is considered to be distributed equally through all available breeding sites and variability between breeding sites in neglected, supported by [67] who noted that females avoid ponds that are overcrowded with existing larvae.

In addition to pond dimension the other important parameter of water bodies is the temperature of the water near the surface. The Depinay model [13] developed a complex empirical function for water temperature as a function of ambient relative humidity and water body size. As the VECTRI model is applied regionally, specific information about individual water body size can not be included. The temperature in shallow ponds and puddles is homogeneous to a good approximation and is often one or two degrees warmer than the air temperature [68, 69]. VECTRI therefore assumes that the temperature of pools T_{wat} to have a fixed offset relative to the air temperature. The default value adopted is a positive offset of 2 K, however, in hot locations it is likely that vector will preferentially choose shaded breeding locations and a lower or even negative offset may be more appropriate. If accurate gridded weather information for wind and surface radiation were available, this aspect of the model could be potential improved implementing a single energy balance model along the lines of [70, 71]. While larger permanent water bodies such as lakes and rivers can have complex stratification of the vertical temperature profile, as discussed above, larvae development occurs mostly in the shallow waters and pools that form on the lake/river boundaries and thus the temperature relation for the permanent water fraction is treated in the same way as the temporary ponds.

References

[1] Hoshen, M. B. & Morse, A. P. A weather-driven model of malaria transmission. *Malar J* **3**, 32, doi:10.1029/2012GL054040 (2004).

[2] Gillies, M. T. Studies on the dispersion and survival of *Anopheles gambiae* Giles in East Africa, by means of marking and release experiments. *Bull Entomol Res* **52**, 99–127 (1961).

[3] Rowley, W. A. & Graham, C. L. The effect of age on the flight performance of female *Aedes aegypti* mosquitoes. *J Insect Physiol* **14**, 719–728 (1968).

[4] Thomson, M. C. *et al.* Movement of *Anopheles gambiae sl* malaria vectors between villages in The Gambia. *Med Vet Entomol* **9**, 413–419 (1995).

[5] Detinova, T. S. *Age-grouping methods in Diptera of medical importance with special reference to some vectors of malaria.* Monograph Series (WHO, 1962).

[6] Jepson, W. F., Moutia, A. & Courtois, C. The malaria problem in Mauritius: The binomics of Mauritian anophelines. *Bull Entomol Res* **38**, 177–208 (1947).

[7] Bayoh, M. N. & Lindsay, S. W. Effect of temperature on the development of the aquatic stages of *Anopheles gambiae sensu stricto* (Diptera: Culicidae). *Bull Entomol Res* **93**, 375–381 (2003).

[8] Ermert, V., Fink, A. H., Jones, A. E. & Morse, A. P. Development of a new version of the liverpool malaria model. i. refining the parameter settings and mathematical formulation of basic processes based on a literature review. *Malar J* **10**, doi:10.1186/1475–2875–10–35 (2011).

[9] Lyimo, E. O., Takken, W. & Koella, J. C. Effect of rearing temperature and larval density on larval survival, age at pupation and adult size of *Anopheles gambiae*. *Entomol Exp Appl* **63**, 265–271 (1992).

[10] Kirby, M. J. & Lindsay, S. W. Effect of temperature and inter-specific competition on the development and survival of *Anopheles gambiae sensu stricto* and *Anopheles arabiensis* larvae. *Acta Trop* **109**, 118–123 (2009).

[11] Bomblies, A., Duchemin, J. B. & Eltahir, E. A. B. Hydrology of malaria: Model development and application to a Sahelian village. *Water Resour Res* **44**, W12445, doi:10.1029/2008WR006917 (2008).

[12] Armstrong, J. A. & Bransby-Williams, W. R. The maintenance of a colony of *Anopheles gambiae*, with observations on the effects of changes in temperature. *Bull World Health Organ* **24**, 427–435 (1961).

[13] Depinay, J. M. O. *et al.* A simulation model of African *Anopheles* ecology and population dynamics for the analysis of malaria transmission. *Malar J* **3**, doi:10.1186/1475–2875–3–29 (2004).

[14] Martens, W. J. M., Niessen, L. W., Rotmans, J., Jetten, T. H. & McMichael, A. J. Potential Impact of Global Climate Change on Malaria Risk. *Environ Health Perspect* **103**, 458–464 (1995).

[15] Thomson, M. C., Mason, S. J., Phindela, T. & Connor, S. J. Use of rainfall and sea surface temperature monitoring for malaria early warning in Botswana. *Am J Trop Med Hyg* **73**, 214–221 (2005).

[16] Paaijmans, K. P., Wandago, M. O., Githeko, A. K. & Takken, W. Unexpected high losses of *Anopheles gambiae* larvae due to rainfall. *PLoS ONE* **2**, e1146, doi:10.1371/journal.pone.0001146 (2007).

[17] Muirhead-Thomson, R. C. The ecology of vector snail habitats and mosquito breeding-places: The experimental approach to basic problems. *Bull World Health Organ* **19**, 637–659 (1958).

[18] Le Menach, A. *et al.* An elaborated feeding cycle model for reductions in vectorial capacity of night-biting mosquitoes by insecticide-treated nets. *Malar J* **6**, 10, doi:10.1186/1475–2875–6–10 (2007).

[19] Ermert, V., Fink, A. H., Jones, A. E. & Morse, A. P. Development of a new version of the Liverpool Malaria Model. II. Calibration and validation for West Africa. *Malar J* **10**, 62, doi:10.1186/1475–2875–10–62 (2011).

[20] Lyimo, E. O. & Takken, W. Effects of adult body size on fecundity and the pre-gravid rate of *Anopheles gambiae* females in Tanzania. *Med Vet Entomol* **7**, 328–332 (1993).

[21] Hogg, J. C., Thompson, M. C. & Hurd, H. Comparative fecundity and associated factors for two sibling species of the *Anopheles gambiae* complex occuring sympatrically in The Gambia. *Med Vet Entomol* **10**, 385–391 (1996).

[22] Takken, W., Klowden, M. J. & Chambers, G. M. Effect of body size on host seeking and blood meal utilization in *Anopheles gambiae* sensu stricto (Diptera: Culicidae): the disadvantage of being small. *J Med Entomol* **35**, 639–645 (1998).

[23] Smith, D. L., Dushoff, J., Snow, R. W. & Hay, S. I. The entomological inoculation rate and *Plasmodium falciparum* infection in African children. *Nature* **438**, 492–495 (2005).

[24] Smith, D. L., McKenzie, F. E., Snow, R. W. & Hay, S. I. Revisiting the basic reproductive number for malaria and its implications for malaria control. *PLoS biol* **5**, e42, doi:10.1371/journal.pbio.0050042 (2007).

[25] Martens, W. J. M., Jetten, T. H., Rottmans, J. & Niessen, L. W. Climate change and vector-borne diseases: A global modelling perspective. *Glob Environ Change* **5**, 195–209 (1995).

[26] Martens, W. J. M., Jetten, T. H. & Focks, D. A. Sensitivity of Malaria, Schistomiasis and Dengue to Global Warming. *Clim Change* **35**, 145–156 (1997).

[27] Craig, M. H., Snow, R. W. & le Sueur, D. A climate-based distribution model of malaria transmission in sub-Saharan Africa. *Parasitol Today* **15**, 105–111 (1999).

[28] Lunde, T. M., Korecha, D., Loha, E., Sorteberg, A. & Lindtjørn, B. A dynamic model of some malaria-transmitting anopheline mosquitoes of the

Afrotropical region. I. Model description and sensitivity analysis. *Malar J* **12**, doi:10.1186/1475–2875–12–28 (2013).

[29] Linard, C., Gilbert, M., Snow, R. W., Noor, A. M. & Tatem, A. J. Population distribution, settlement patterns and accessibility across Africa in 2010. *PLoS ONE* **7**, e31743, doi:10.1371/journal.pone.0031743 (2012).

[30] Balk, D. L. *et al.* Determining global population distribution: methods, applications and data. *Adv Parasitol* **62**, 119–156 (2006).

[31] Dekker, T., Steib, B., Carde, R. T. & Geier, M. L-lactic acid: a human-signifying host cue for the anthropophilic mosquito *anopheles gambiae*. *Med Vet Entomol* **16**, 91–98 (2002).

[32] Mahande, A., Mosha, F., Mahande, J. & Kweka, E. Feeding and resting behaviour of malaria vector, *Anopheles arabiensis* with reference to zooprophylaxis. *Malar J* **6**, 100, doi:10.1186/1475–2875–6–100 (2007).

[33] Killeen, G. F., McKenzie, F. E., Foy, B. D., Bøgh, C. & Beier, J. C. The availability of potential hosts as a determinant of feeding behaviours and malaria transmission by African mosquito populations. *Trans R Soc Trop Med Hyg* **95**, 469–476 (2001).

[34] Bøgh, C., Clarke, S. E., Pinder, M., Sanyang, F. & Lindsay, S. W. Effect of passive zooprophylaxis on malaria transmission in The Gambia. *J Med Entomol* **38**, 822–828 (2001).

[35] Koella, J. C., SÖrensen, F. L. & Anderson, R. A. The malaria parasite, *Plasmodium falciparum*, increases the frequency of multiple feeding of its mosquito vector, *Anopheles gambiae*. *Proc R Soc Lond B Biol Sci* **265**, 763–768 (1998).

[36] Lindsay, S. W., Adiamah, J. H., Miller, J. E., Pleass, R. J. & Armstrong, J. R. M. Variation in attractiveness of human subjects to malaria mosquitoes (Diptera: Culicidae) in The Gambia. *Journal of medical entomology* **30**, 368–373 (1993).

[37] Knols, B. G. J., de Jong, R. & Takken, W. Differential attractiveness of isolated humans to mosquitoes in Tanzania. *Trans R Soc Trop Med Hyg* **89**, 604–606 (1995).

[38] Mukabana, W. R., Takken, W., Coe, R. & Knols, B. G. J. Host-specific cues cause differential attractiveness of Kenyan men to the African malaria vector *Anopheles gambiae*. *Malar J* **1**, 17, doi:10.1186/1475–2875–1–17 (2002).

[39] Lwetoijera, D. W. *et al.* A need for better housing to further reduce indoor malaria transmission in areas with high bed net coverage. *Parasit Vectors* **6**, 57 (2013).

[40] Carter, R., Mendis, K. N. & Roberts, D. Spatial targeting of interventions against malaria. *Bull World Health Organ* **78**, 1401–1411 (2000).

[41] Bousema, T. *et al.* Hitting hotspots: spatial targeting of malaria for control and elimination. *PLoS medicine* **9**, e1001165. doi:10.1371/journal.pmed.1001165 (2012).

[42] Kienberger, S. & Hagenlocher, M. Spatial-explicit modeling of social vulnerability to malaria in East Africa. *International journal of health geographics* **13**, 29 (2014).

[43] Lacroix, R., Mukabana, W. R., Gouagna, L. C. & Koella, J. C. Malaria infection increases attractiveness of humans to mosquitoes. *PLoS Biol* **3**, e298 (2005).

[44] Dye, C. & Hasibeder, G. Population dynamics of mosquito-borne disease: effects of flies which bite some people more frequently than others. *Trans R Soc Trop Med Hyg* **80**, 69–77 (1986).

[45] Shute, P. G. & Maryon, M. A study of gametocytes in a West African strain of *Plasmodium falciparum*. *Trans R Soc Trop Med Hyg* **44**, 421–438 (1951).

[46] Miller, M. J. Observations on the natural history of malaria in the semi-resistant West African. *Trans R Soc Trop Med Hyg* **52**, 152–168 (1958).

[47] Hawking, F., Wilson, M. E. & Gammage, K. Evidence for cyclic development and short-lived maturity in the gametocytes of *Plasmodium falciparum*. *Trans R Soc Trop Med Hyg* **65**, 549–555 (1971).

[48] Day, K. P., Hayward, R. E. & Dyer, M. The biology of *Plasmodium falciparum* transmission stages. *Parasitol* **116 (Suppl.)**, S95–S109 (1998).

[49] Doolan, D. L., Dobano, C. & Baird, J. K. Acquired immunity to malaria. *Clin Microbiol Rev* **22**, 13, doi:10.1128/CMR.00025–08 (2009).

[50] Laneri, K. *et al.* Forcing versus feedback: epidemic malaria and monsoon rains in northwest India. *PLoS Comput Biol* DOI: 10.1371/journal.pcbi.1000898 (2010).

[51] Filipe, J. A. N., Riley, E. M., Drakeley, C. J., Sutherland, C. J. & Ghani, A. C. Determination of the processes driving the acquisition of immunity to malaria using a mathematical transmission model. *PLoS Comput Biol* **3**, e255, doi:10.1371/journal.pcbi.0030255 (2007).

[52] Klein, E. Y., Smith, D. L., Boni, M. F. & Laxminarayan, R. Clinically immune hosts as a refuge for drug-sensitive malaria parasites. *Malar J* **7**, 1 (2008).

[53] Boudin, C. *et al.* *Plasmodium falciparum* transmission blocking immunity in three areas with perennial or seasonal endemicity and different levels of transmission. *Am J Trop Med Hyg* **73**, 1090–1095 (2005).

[54] Le Prince, J. A. Mosquito control in relation to impounded water supply. *J Am Water Works Assoc* **17**, 31–36 (1927).

[55] Fillinger, U. *et al.* Identifying the most productive breeding sites for malaria mosquitoes in The Gambia. *Malar J* **8**, doi:10.1186/1475–2875–8–62 (2009).

[56] Haque, U. *et al.* The role of climate variability in the spread of malaria in Bangladeshi highlands. *PLoS ONE* **5**, e14341, doi:10.1371/journal.pone.0014341 (2010).

[57] Desconnets, J. C., Taupin, J., Lebel, T. & Leduc, C. Hydrology of the hapex-sahel central super-site: surface water drainage and aquifer recharge through the pool systems. *Journal of Hydrology* **188**, 155–178 (1997).

[58] Gianotti, R. L., Bomblies, A. & Eltahir, E. A. B. Hydrologic modeling to screen potential environmental management methods for malaria vector control in Niger. *Water Resour Res* **45**, W08438, doi:10.1029/2008WR007567 (2009).

[59] Martin-Rosales, W. & Leduc, C. Dynamiques de vidange d'une mare temporaire au sahel: l'exemple de banizoumbou (sud-ouest du niger). *Comptes Rendus Geoscience* **335**, 461–468 (2003).

[60] Hayashi, M. & Van der Kamp, G. Simple equations to represent the volume–area–depth relations of shallow wetlands in small topographic depressions. *Journal of Hydrology* **237**, 74–85 (2000).

[61] Brooks, R. T. & Hayashi, M. Depth-area-volume and hydroperiod relationships of ephemeral (vernal) forest pools in southern new england. *Wetlands* **22**, 247–255 (2002).

[62] Soti, V. *et al.* The potential for remote sensing and hydrologic modelling to assess the spatio-temporal dynamics of ponds in the Ferlo Region (Senegal). *Hydrol Earth Sys Sci Discuss* **14**, 1449–1464 (2010).

[63] Alonso, D., Bouma, M. J. & Pascual, M. Epidemic malaria and warmer temperatures in recent decades in an East African highland. *Proc R Soc Lond B Biol Sci* **278**, 1661–1669 (2011).

[64] Eckhoff, P. A. A malaria transmission-directed model of mosquito life cycle and ecology. *Malar J* **10**, 10, doi:10.1186/1475–2875–10–303 (2011).

[65] Wanjala, C. L., Githeko, A. K. & Waitumbi, J. N. Assessing the impact of topography on malaria exposure and malaria epidemic sensitivity in the Western Kenya highlands. *Malar J* **9(Suppl. 2)**, P59, doi: 10.1186/1475–2875–9–S2–P59 (2010).

[66] Gimnig, J. E. *et al.* Density-dependent development of *Anopheles gambiae* (Diptera: Culicidae) larvae in artificial habitats. *J Med Entomol* **39**, 162–172 (2002).

[67] Munga, S. *et al.* Effects of larval competitors and predators on oviposition site selection of *Anopheles gambiae sensu stricto*. *J Med Entomol* **43**, 221–224 (2006).

[68] Paaijmans, K. P. *et al.* Observations and model estimates of diurnal water temperature dynamics in mosquito breeding sites in western Kenya. *Hydrol Process* **22**, 4789–4801 (2008).

[69] Paaijmans, K. P., Takken, W., Githeko, A. K. & Jacobs, A. F. G. The effect of water turbidity on the near-surface water temperature of larval habitats of the malaria mosquito *Anopheles gambiae*. *Int J Biometeorol* **52**, 747–753 (2008).

[70] Jacobs, A. F. G., Heusinkveld, B. G., Kraai, A. & Paaijmans, K. P. Diurnal temperature fluctuations in an artificial small shallow water body. *Int J Biometeorol* **52**, 271–280 (2008).

[71] Paaijmans, K. P., Heusinkveld, B. G. & Jacobs, A. F. G. A simplified model to predict diurnal water temperature dynamics in a shallow tropical water pool. *Int J Biometeorol* **52**, 797–803 (2008).

List of constants in VECTRI.

Symbol	Value	Units	Description	
$E + I$	250	mm day^{-1}	total evaporation and infiltration losses	
$K_{L,jepson}$	90.9	K day	Larvae growth degree days	
$K_{L,Bayoh}$	200	K day	Larvae growth degree days	
K_{gono}	37.1	K day	Gonotrophic cycle degree days	
K_{sporo}	111	K day	Sporogonic cycle degree days	
$K_{flush,\infty}$	0.4		Larvae flushing factor for infinite rainrate	
K_w	1	m	pond growth rate factor	set by tun
$K_{mar1,0}$	0.45		constant of Martens I vector survival scheme	
$K_{mar1,1}$	0.054	K^{-1}	constant of Martens I vector survival scheme	
$K_{mar1,2}$	-0.0016	K^{-2}	constant of Martens I vector survival scheme	
$K_{mar2,0}$	-4.4		constant of Martens II vector survival scheme	
$K_{mar2,1}$	1.31	K^{-1}	constant of Martens II vector survival scheme	
$K_{mar2,2}$	-0.03	K^{-2}	constant of Martens II vector survival scheme	
$M_{L,max}$	300	mg m^{-2}	Carrying capacity of water bodies	
N_{egg}	120		Number of eggs per batch that result in female vectors	
$P_{L,surv_0}$	0.825		Larvae base daily survival rate	
P_{hv}	0.2		probability of transmission from infective host to vector during single bloodmeal	
P_{vh}	0.3		probability of transmission from infective vector to host during single bloodmeal	
S_{ie}	4×10^{-6}	day^{-1}	Pond evaporation/infiltration sink	
T_{wat}	$T_2m + 2$	K	Pond water temperature	
$T_{L,min}$	16	K	minimum T_{wat} for larvae development	
$T_{L,max}$	38	K	maximum T_{wat} for larvae development	
$T_{gono,min}$	7.7	K	minimum T_{2m} for egg development	
$T_{sporo,min}$	16	K	minimum T_{2m} for sporogonic cycle	
τ_{flush}	50	mm day^{-1}	Larvae-flushing rainfall e-folding factor	
τ_{zoo}	50	km^{-2}	population density zoophilic factor	
w_{max}	0.04		maximum temporary pond fraction in cell	set by tun